18TH WORLD CONFERENCE ON EARTHQUAKE ENGINEERING
WCEE2024
MILAN

MILAN, ITALY
30TH JUNE - 5TH JULY 2024
www.wcee2024.it

SEISMIC PERFORMANCE OF FIRE-DAMAGED STRUCTURES: PRELIMINARY ANALYSIS OF A 14-STOREY CASE STUDY STRUCTURE

S. Dede[1], T. Rossetto[2] & F. Freddi[3]

[1] Research Student, EPICentre, University College London, London, U.K. sahin.dede.21@ucl.ac.uk

[2] Professor, EPICentre, University College London, London, U.K.

[3] Associate Professor, EPICentre, University College London, London, U.K.

Abstract: *Urban fires represent one of the major disasters frequently occurring in densely populated built environments. Except for rare cases of extreme residential fires leading to visible structural damage, reinstating the aesthetic appearance of the building without in-depth structural investigations is a widely followed practice for most fire-damaged buildings. Such a scenario does not generally jeopardise the daily service of the building thanks to the safety coefficients adopted in the gravity design. However, this may significantly affect the response and safety of buildings located in seismically active regions. The city of Istanbul is expecting a large earthquake in the near future and regularly suffers from thousands of residential fires annually, as revealed by the statistics of the Istanbul Fire Brigade. To investigate the effects of fire damage on the seismic response of building structures, the present paper numerically evaluates the seismic performance of an existing high-rise tunnel-form building, considering several fire damage scenarios of increasing intensity and progressive spread. Tunnel-form buildings are a popular typology used in mass housing projects in Turkey and are widespread across the country. A 14-storey tunnel-form building constructed in Istanbul is considered for case study purposes, and a state-of-the-art 3D finite element model of the case study building is developed in OpenSeesPY to carry out the numerical simulations. Numerical models are developed for the original undamaged structure and for several post-fire scenarios. Varying levels of deterioration caused by the intensity and spread of fire scenarios are reflected at material and section levels within the finite element models. Changes in the seismic response are investigated through nonlinear time history analyses performed on the undamaged and fire-damaged structures. The outcomes of this preliminary study present the increased seismic vulnerability in the post-fire state and highlight the impacts of the fire scenarios on different structural response parameters.*

1. Introduction

Extending parallel to the unruptured segment of the North Anatolian Fault (NAF), Istanbul is expecting a large-magnitude earthquake in the near future. Along with this significant earthquake hazard, the city's residential building stock is suffering more than five thousand fire incidents every year, as documented by the annual data provided by the Istanbul Fire Department (2008-2022). Although severe fire incidents lead residents and authorities to consult with engineers for a detailed engineering investigation, including material testing and damage assessments, these procedures are often ignored after small- to medium-sized fires. As damage is less visible in such cases, the urgency of residents and/or owners is typically on restoring the aesthetic appearance of the fire-affected area to reoccupy the building. This often results in unrepaired damage

remaining hidden within the affected area. Economic concerns of the residents to conduct an extensive engineering investigation and over-confidence in the fire performance of reinforced concrete, which is by far the dominant construction material in Istanbul, often lead to neglect in-depth structural assessments after small to medium fires. However, as demonstrated by Ioannou *et al.* (2022), even short-duration fires can have adverse effects on the behaviour of reinforced concrete members and, therefore, on the structure as a whole. The concrete core and the reinforcing steel can be affected by such short-duration fires due to the heat transfer mechanism (Ioannou *et al.* 2022; Melo *et al.* 2022; Demir *et al.* 2020), resulting in stiffness and strength degradation and the consequent reduction of ductility and energy dissipation capacities. Safety factors used in the design provide a safety buffer for the service/daily use of buildings damaged by small to medium-sized fires, as the degree of strength reduction in structural RC elements does not pose a significant threat in such cases. However, it is unclear to what extent such fire damage affects the seismic performance of structures.

Several studies (*e.g.,* Parsons *et al.* 2000; Erdik *et al.* 2003) estimated that the probability of occurrence of a 7.0+ magnitude earthquake in Istanbul is very high. Additionally, the cumulative increase of fire-damaged buildings may create a seismically more vulnerable group of buildings. Such buildings may pose a significant issue for Istanbul, albeit research into the seismic response of fire-damaged buildings in the city has received limited attention.

The present paper shares a preliminary investigation of the post-fire seismic behaviour of a Turkish RC tunnel-form building considering several fire scenarios with different severity and extend. Tunnel-form buildings are the main typology preferred for mass housing projects in Turkey. Moreover, given the satisfactory performance demonstrated during the February 2023 Turkey earthquakes, it is expected that they will occupy more spaces in urban environments. As a result of their distinct construction technique, these buildings have very similar features. In this paper, a 14-storey tunnel-form building is selected and modelled in OpenSeesPY (Zhu *et al.* 2018) to investigate its post-fire seismic response. Material and section properties of fire-exposed members are modelled accordingly for each fire scenario. The reference model (*i.e.,* with no fire damage) and three post-fire damaged cases have been subjected to a ground motion record to investigate the influence of the fire damage on the seismic response. The impact of fire severity and extent are presented and critically discussed.

2. Case study structure and finite element modelling

2.1 Case study structure

An existing 14-storey residential tunnel-form building sharing the same height, plan and design with hundreds of others across Istanbul is selected as the case study to evaluate their post-fire seismic performance. Plan and elevation views of the case study building are provided in Figure 1. Any active fire protection system is not installed, and specific protective measurements such as fire doors and protective paints are not applied within the actual building. A particular building in Istanbul is used for the numerical model because of its accessibility for conducting ambient vibration measurements to verify the modal properties of the numerical model.

Figure 1. (A) Floor plan and (B) elevation view of the case study structure.

The case study building has identical floor plans throughout its height, 27.0 m × 21.6 m in plan with 520 m^2 of floor area. 6.44% of the floor area is composed of 26 thin sectioned shear walls with 0.2 m thickness. Moreover, the vertical load-bearing system includes 12 columns with three different section dimensions equal to 0.2 m × 0.2 m, 0.2 m × 0.95 m, and 0.2 m × 1.25 m. Loads are transferred among these members by 27 beams with varying depths and 0.15 m thick slabs. The total height of the building is 39.2 m, and each storey has a height of 2.8 m, including the basement surrounded by continuous exterior shear walls.

The seismic design of the building was realised as per the Turkish Building Seismic Code 2007 (TBSC 2007). The compressive strength of the concrete used for all structural components is 30 MPa. Steel rebars within the shear wall boundary regions, columns, beams, and slabs have a yield strength of 420 MPa, whereas steel rebars within the shear wall web regions are mesh reinforcements with a yield strength of 500 MPa. Specifications provided for high-ductility members are followed to design all structural members. Throughout the critical height of the building, which only includes ground- and first-storey, the reinforcement ratios of shear walls range between 0.4%-0.7%, while the shear walls in the rest of the building have reinforcement ratios between 0.3%-0.6%. Many of the shear walls that are aligned parallel to the long direction of the building are coupled through conventionally reinforced deep coupling beams with span-to-depth ratios of less than 2.

2.2 Finite element modelling

OpenSeesPY (Zhu *et al.* 2018) is utilised to create a state-of-the-art finite element model of the case study building. Shear walls and wall-like columns are represented by line elements following the wide-column analogy where section centroids are linked to the adjacent nodes by stiff, elastic beams. The inelastic behaviour of the structure is captured at the shear wall, column, and beam levels by modelling them with 'nonlinearBeamColumn' elements, which adopt a fibre-based distributed plasticity approach. Constitutive relationships of both unconfined and confined concrete are represented by the 'Concrete01' material model. The stress-strain relationship of confined concrete material is estimated according to Mander *et al.* (1988). The stress-strain relationships of steel reinforcements with f_y=420 MPa and f_y=500 MPa are represented by the 'Steel02' material. Material nonlinearity is inherently considered by means of the aforementioned material models, whereas geometric nonlinearity is explicitly defined by 'PDelta' coordinate transformation command.

Fibre-based modelling is a computationally efficient technique and is considered a suitable approach to capture the flexural response of slender shear walls. Although slender shear walls undergo significant flexural demands, it has been observed in post-earthquake field observations and experimental campaigns that mainly fail under concrete crushing, reinforcement buckling, and reinforcement fracture (Wallace 2012; Pugh *et al.* 2015). Since almost all of the vertical load-bearing members in tunnel-form buildings are shear walls, their accurate finite element modelling is crucial to capture not only the local but also the global response. However, fibre-based elements cannot directly simulate the aforementioned brittle failures (concrete crushing, reinforcement buckling, and reinforcement fracture), and some modifications are required. In particular, to capture these failure modes, materials are modified to exhibit rapid strength loss after exceeding certain strain threshold values. The buckling strain of steel rebars is equal to the crushing strain of neighbouring concrete fibres, defined as the strain at which the concrete experiences an 80% loss of its peak strength. At the same time, the rupture strain of steel rebars under tension is taken as 5% tensile strain (Pugh *et al.* 2015; Gogus and Wallace 2015). Moreover, the material regularisation technique provided by Pugh *et al.* (2015) is adopted to overcome strain localisation phenomena occurring due to the force-based integration scheme. Bilinear shear force-deformation relationships are defined for each shear wall, column, and beam to define an uncoupled shear response at the section level adopting 'Hysteretic' material. Elastic membrane plate elements are used to model slabs and peripheral basement walls. Cracked section stiffness reduction factors of 25% and 50%, for slabs and peripheral basement walls, respectively, are applied according to common practice (TBSC 2018; ACI 318-14). Dead loads, live loads, and self-weight of the system are used as the mass source of the structural system. Calculated masses are applied to the joints at each floor level.

The strategies followed to model structural members have already been validated in literature, and in this study such methods are merged to create a detailed 3D finite element model of a complex high-rise structure. An ambient vibration measurement campaign was conducted on the existing case study building to identify the fundamental frequencies and then compare them against those of the finite element model. For the sake of brevity, an in-depth discussion about signal processing is not provided in this paper. Ambient vibration measurements have shown that the first three fundamental periods of the building span between 1.7 and 2.0 Hz; the first mode is torsional, while the second and third modes are orthogonal, having very close frequencies.

The first three fundamental frequencies of the finite element model with and without stiffness modification factors applied are provided in Table 1. The latter, which disregards any crack that may occur during severe shakings, is used to compare against the field measurement data as ambient vibrations are low amplitude motions within the elastic range.

Table 1. Fundamental periods of the case study structure.

Mode	Finite element model without cracked section stiffness	Finite element model with cracked section stiffness
First Mode (Torsional)	0.52 s (1.92 Hz)	0.64 s (1.56 Hz)
Second Mode (Translational X)	0.50 s (2.00 Hz)	0.58 s (1.72 Hz)
Third Mode (Translational Y)	0.48 s (2.08 Hz)	0.55 s (1.82 Hz)

2.3 Implementation of fire damage

Degradations in the mechanical properties of concrete and steel due to elevated temperatures need to be reflected in the finite element model, as any change in the material behaviour alters the response of the member. In this study, linear and nonlinear responses of the building are represented through fibre-based elements in which constitutive relationships of uniaxial material models along with the bilinear shear force-deformation relationships of fibre sections form the basis. To reflect the post-fire state of the building, material models and shear springs are modified according to the considered fire scenarios presented in the next section. Herein, the framework proposed by Ioannou *et al.* (2022) is followed to reflect the post-fire material behaviour. Ioannou *et al.* (2022) investigated the post-fire cyclic behaviour of 0.30 m square pre-code columns and presented experimentally validated material models. Although the experimented structural member in Ioannou *et al.* (2022) is not representative of the shear walls, the framework is sufficient for the preliminary investigation of the case study building as being the shear walls very thin (0.20 m), the heat can be assumed to be fully transferred from one side to the other side of the element. Thus, the coefficients representing the post-fire strength, stiffness, and ductility degradation in Ioannou *et al.* (2022) are applied to the shear walls and columns of the case study building, considering the fire scenarios. Being the main components contributing to the stability of the structure, such modification factors are applied only to the vertical members. In addition to the material constitutive relationships, bilinear shear force-deformations are altered based on the corresponding material modifications. All fibre sections of fire-exposed members have the same material models and shear springs since a uniform heat distribution assumption within each compartment is adopted (BS EN 1991 1-2; Buchanan and Abu 2017).

3. Seismic performance assessment of fire-damaged structures

The post-fire seismic response of the case study structure was investigated by comparing the response from a total of four 3D finite element models representing three different fire damage scenarios in addition to the reference model with no previous fire damage. For simplicity, the fire hazard is not explicitly modelled in this preliminary investigation. Instead, it is assumed that a fire incident occurred within the service life of the building, and the fire-affected areas did not receive any engineering treatment. Three different fire scenarios are considered, and Figure 2 shows the floor plan and flat numbers that are used to define each fire scenario. Each flat is identical, has a floor area of 100 $m^{2,}$ and does not contain any active fire protection system or fireproofing measures.

Table 2 summarises the scenarios used in terms of distribution and duration for each flat. The durations provided in Table 2, do not reflect the real time of the fire event but are the quantified effect of fire on material characteristics as discussed in the experimental study of Melo *et al.* (2022) and utilised by Ioannou *et al.* (2022). Fire durations are defined as per BS EN 1991 1-2 and based on ISO-834 time-temperature curves. Although these curves do not represent real fires, they are the primary practice in fire rating tests and form a common language in fire engineering (Buchanan and Abu 2017). As a result, Table 2 presents the scenarios and quantified fire damage considered in that specific scenario.

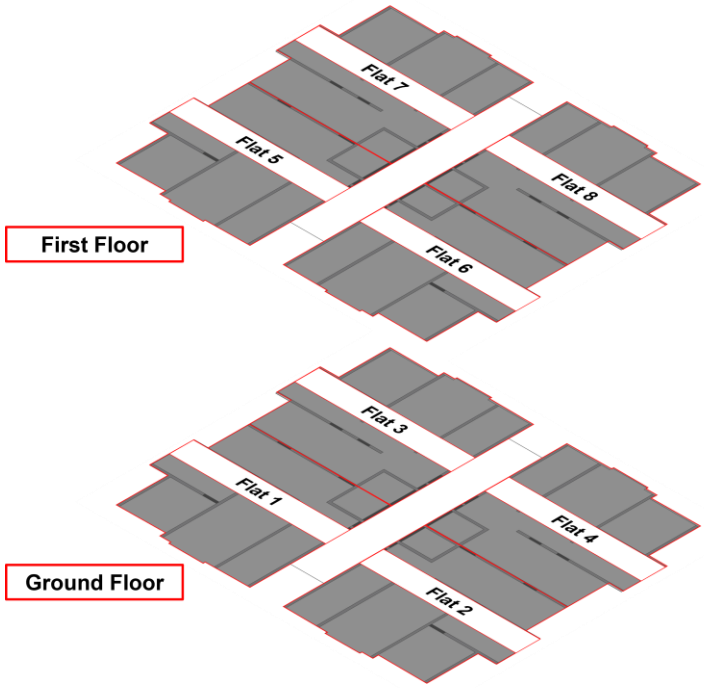

Figure 2. Schematic view of ground and first floors

Table 2. Scenario for fire damage in terms of distribution and duration in minutes.

Scenario	Ground Floor				First Floor			
	Flat 1	Flat 2	Flat 3	Flat 4	Flat 5	Flat 6	Flat 7	Flat 8
O	-	-	-	-	-	-	-	-
A	30	-	-	-	-	-	-	-
B	90	60	60	30	30	-	-	-
C	90	90	90	90	90	90	90	90

The reference model with no prior damage is covered by Scenario O. Scenario A represents the least severe case where a fire incident occurred within Flat 1, and caused the equivalent of 30 minutes of fire damage. Scenario B represents a more severe situation with more intense damage and a larger spread. The same applies to Scenario C, which is the most severe situation considered. Tables 3 and 4 provide the coefficients used to modify the material properties considering the quantified fire damage. The shear walls and columns in the fire-damaged apartments of the scenarios in Table 2 are modified by considering the coefficients in Tables 3 and 4. The materials of each element are modified with the given coefficients, and then the shear springs are updated. These steps are applied to all vertical elements for each apartment in each scenario, resulting in a total of four different 3D finite element models.

Table 3. Modification factors for fire-damaged concrete material (adapted from Ioannou et al. 2022).

Fire Damage as Minutes	f_{cy}		ε_{cy}		f_{cu}		ε_{cu}	
	Cover Concrete	Core Concrete	Cover Concrete	Core Concrete	Cover Concrete	Core Concrete	Cover Concrete	Core Concrete
No prior damage	1.00	1.00	1.00	1.00	1.00	1.00	1.00	1.00
30	0.64	0.90	1.95	1.00	0.62	0.90	1.06	1.03
60	0.55	0.80	2.50	1.25	0.53	0.81	1.15	1.05
90	0.45	0.71	3.05	1.50	0.44	0.71	1.25	1.07

Table 4. Modification factors for fire-damaged reinforcing steel material (adapted from Ioannou et al. 2022).

Fire Damage as Minutes	f_{sy}	E_s (MPa)	f_{su}	ε_{su}	b_s
No prior damage	1.00	1.00	1.00	1.00	1.00
30	1.00	1.00	1.00	1.03	1.00
60	0.93	0.98	0.94	0.97	1.04
90	0.87	0.97	0.88	0.91	1.09

A single ground motion record reflecting the fault characteristics of the NAF is used to investigate the seismic response of the structure under four different cases. The selected accelerogram was recorded at Yarimca station on the 17th of August 1999 and related to the M_w 7.4 Kocaeli earthquake that occurred on the NAF. TBSC 2007 requires that the accelerations of the selected ground motion record between periods of $0.2T_1$-$2.0T_1$ should be higher than the acceleration values of the site-specific design spectrum over the same period. To satisfy this criterion, the ground motion record is scaled by a factor of 2.4. The two components of the selected ground motion are provided in Figure 3, along with the comparison of its response spectrum against the site-specific design spectrum. Orthogonal components of the ground motion record are simultaneously applied to conduct nonlinear time history analyses of each 3D finite element model.

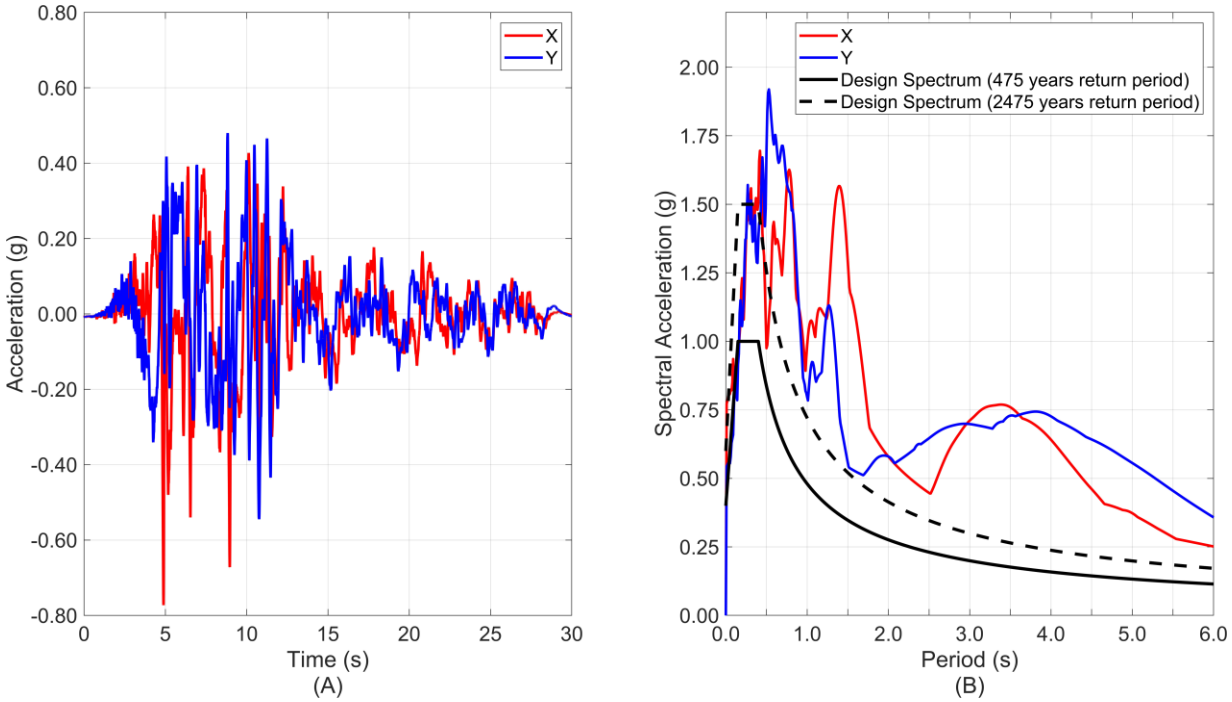

Figure 3. Acceleration record (A) and response spectra (B) of the M_w = 7.4 Kocaeli earthquake

4. Results

The global demand parameters obtained from the nonlinear time history analyses are provided in this chapter. The impact of the progressively intensifying fire scenarios on the modal parameters is examined through the data given in Table 5. The displacement response histories are used to provide insights into the seismic response and are shown in Figures 4 and 5 separately for each direction and as 2D planar motions in orthogonal directions. Lastly, the maximum and residual interstorey drift ratios (IDR) given in Figures 6 and 7 are provided to synthetically evaluate the effects of fire damage along the building height.

Table 5 indicates that even in the worst-case scenario, where two stories experienced the most significant fire damage, the building experienced a period elongation lower than 10%. Also, asymmetric fire spread, like the one simulated in Scenario B, does not significantly affect the torsional mode. These results suggest that local fire damage, even spanning two stories, might not significantly alter the building's modal characteristics compared to its undamaged state. The same holds for the mass participation factors, as there is only a slight

decrease. These findings imply that ambient vibration measurements with the minimum possible installations might not detect a prior damage history.

Table 5. Comparison of modal parameters.

Scenario	First Mode (Torsion)		Second Mode (X)		Third Mode (Y)	
	T (s)	Γ (%)	T (s)	Γ (%)	T (s)	Γ (%)
O	0.63	69.1	0.58	72.4	0.54	68.4
A	0.69	68.5	0.58	72.4	0.55	68.3
B	0.71	68.2	0.60	71.9	0.57	67.9
C	0.73	68.0	0.63	71.4	0.61	67.0

Figure 4 shows that the building exhibits more pronounced oscillations along its longer side (X) compared to the shorter side (Y) during this specific ground motion. Scenario A shows nearly no change from the undamaged state (Scenario O). However, starting from Scenario B, the building experiences severe oscillations and residual displacements in different directions. Examining the displacement responses in Figures 4 and 5 reveals that Scenario B, medium severity but significant asymmetry, causes the most substantial effects along the X direction, and the building suffers a residual displacement of 5.9 cm. This intensified response might be related to the fact that the dominant mode of the building is torsional. In the Y direction, Scenario B, in contrast to the X direction, does not cause the most severe damage; however, it leads to a residual displacement in the opposite direction to the other scenarios due to asymmetric loading.

Figure 6 shows that the ground floor of the building (0.0 to 2.8 meters) in Scenario B exhibits the highest Interstorey Drift Ratios (IDRs). This soft-storey response persists in Scenario A. However, in Scenarios B and C, this response not only shifts to the first floor but also intensifies. Figure 7 supports these observations, showing significant residual IDRs on the first floor (2.8 to 5.6 meters).

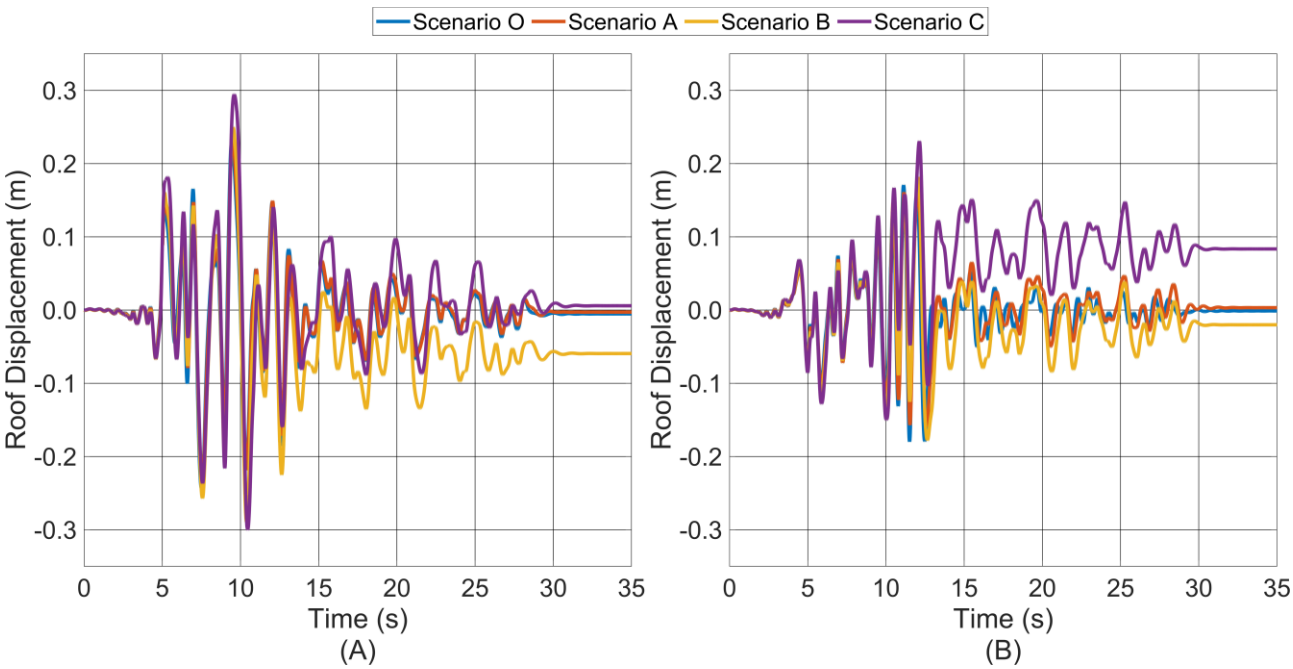

Figure 4. Displacement response of each scenario at the roof mass centroid. (A) X direction (B) Y direction.

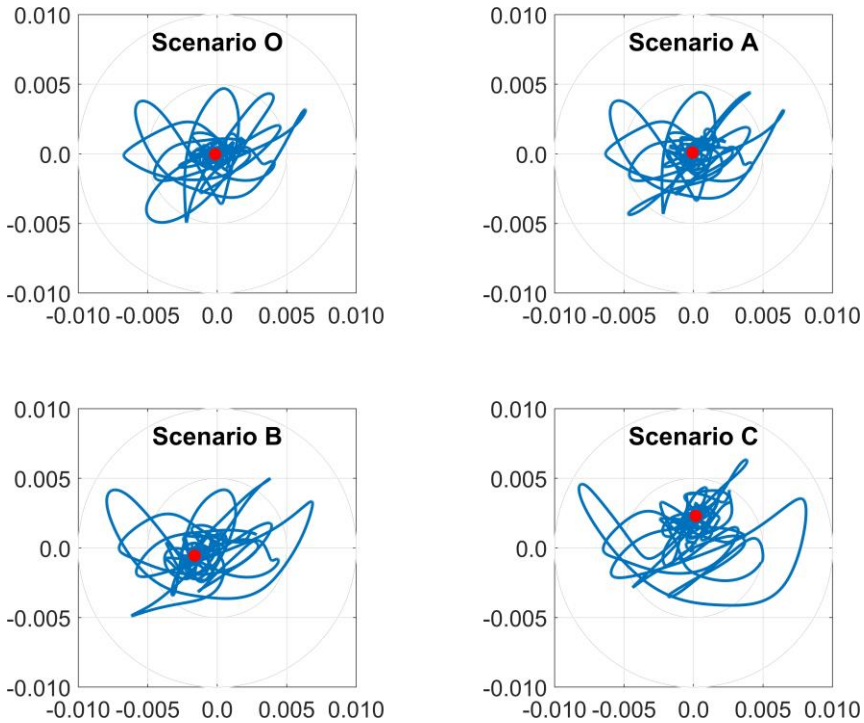

Figure 5. Planar display of displacement response at the roof mass centroid proportioned to the building height above the ground. X direction is the horizontal axis, and Y direction is the vertical axis. Red dot indicates the final displacement of the point.

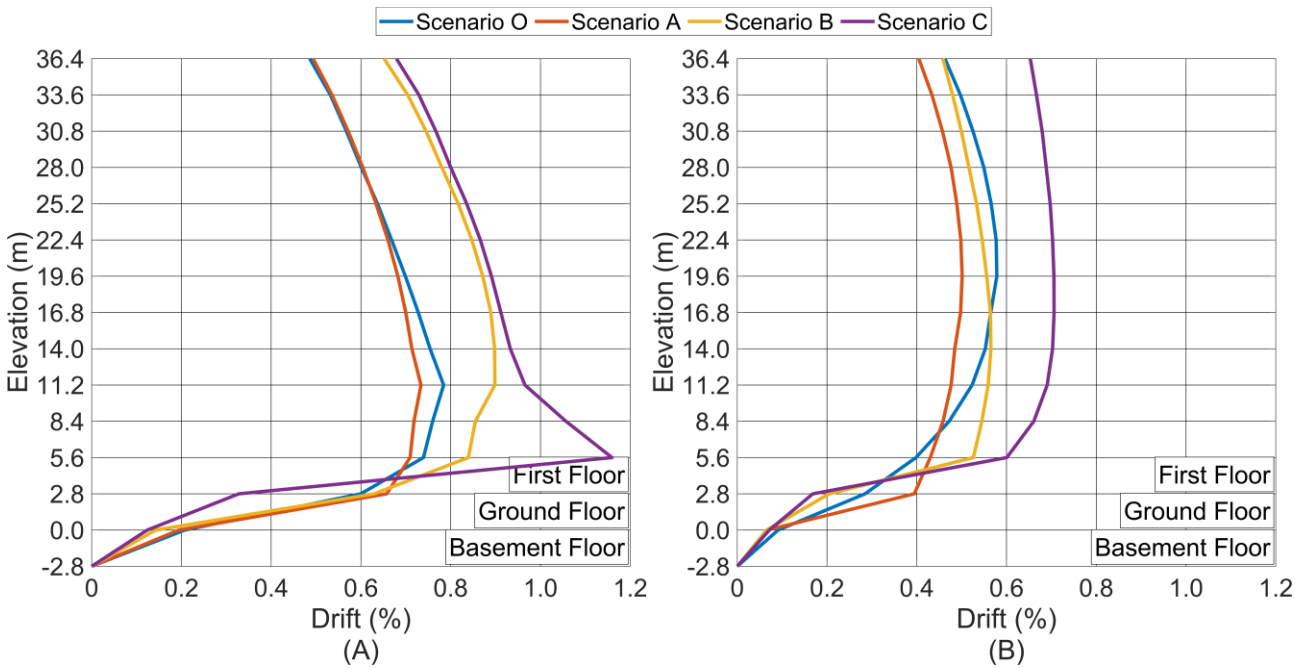

Figure 6. Maximum interstorey drift ratios obtained at mass centroid of each floor for each scenario. (A) X direction (B) Y direction.

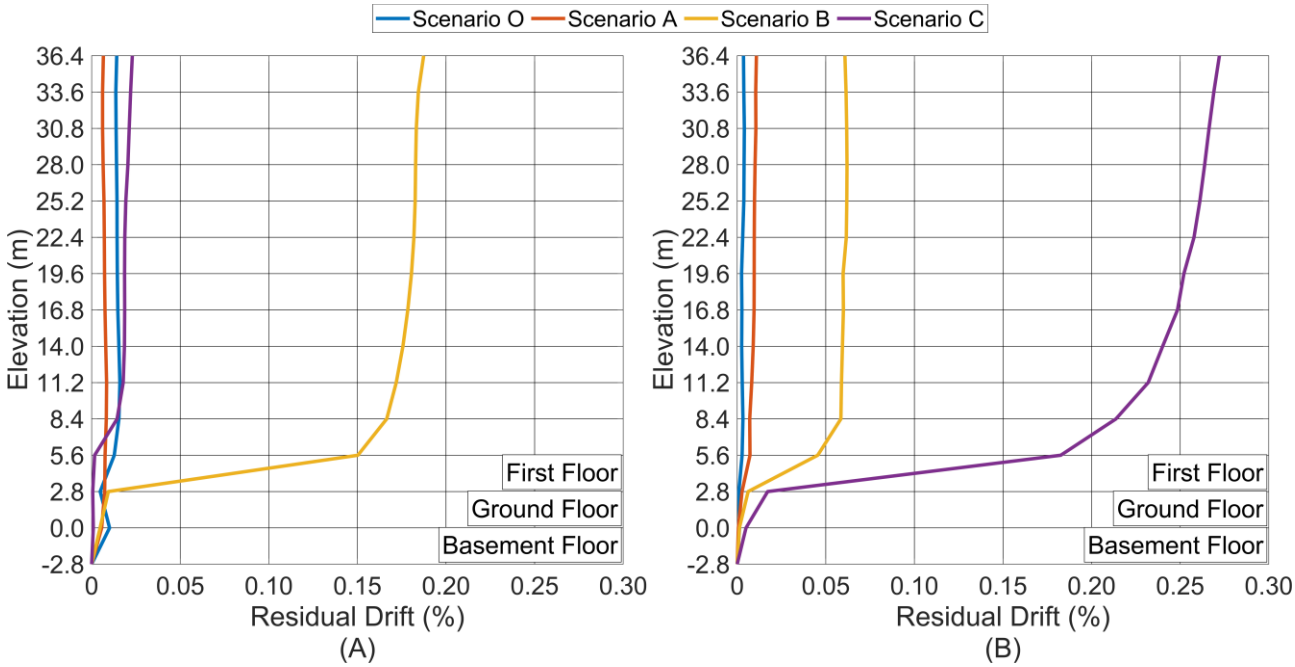

Figure 7. Residual interstorey drift ratios obtained at the roof centroid of each floor for each scenario. (A) X direction (B) Y direction.

5. Conclusion

An index 14-storey tunnel-form building, representing hundreds of others constructed for mass housing projects across Istanbul, is used as a case study to investigate the post-fire seismic response considering several scenarios of small to medium-sized fires. Each subsequent scenario represented a case with an increased severity of fire damage and spread in the building. Fire severity is reflected by the deterioration of strength, stiffness, and ductility at the material level to represent the post-fire state.

Modal analysis results suggest that the progressive fire damage scenarios considered in this study do not signoficantly affect the , natural vibration periods and mass participation ratios. This observation indicates that ambient vibration measurements might npt be adequate tp detect fire damage in buildings that have suffered small to medium-sized fires.

As the extent and intensity of fire increase, the building's oscillations, residual displacements, and interstorey drift ratios increase due to the more severe and widespread damage. The most severe scenario, Scenario C, results in the largest drifts and displacements in the short direction of the structure. Instead, the most asymmetric scenario, Scenario Bcauses more pronounced oscillations and residual drifts along the longer direction of the building. This suggests that the distribution and resulting asymmetry of the post-fire damage and structural layout play a significant role in the post-fire seismic response.

Outcomes of the preliminary numerical investigation on the case study index building indicate that fire damage lead to more pronounced seismic response. The results have also shown that the increased vulnerability is not linearly proportionate to the severity of the fire event. Accordong to fire statistics (REF) more than five thousand fire incidents occur in RC residential buildings each year in Istanbul. Consequently, this study suggests that the accumulation of small- to medium-sized fires creates a more seismic vulnerable building stock. To have a deeper comprehension on the possible consequences of fire on seismic performance, a wider spectrum of fire scenarios should be considered.

6. References

Istanbul Fire Department Statistics (2008-2022). Istanbul Metropolitan Municipality, Turkey.

Ioannou, I., Rossetto, T., Rush, D. and Melo, J. (2022). Simplified model for pre-code RC column exposed to fire followed by earthquake. Scientific reports, 12(1), p.8980.

Melo, J., Triantafyllidis, Z., Rush, D., Bisby, L., Rossetto, T., Arêde, A., Varum, H. and Ioannou, I. (2022). Cyclic behaviour of as-built and strengthened existing reinforced concrete columns previously damaged by fire. Engineering Structures, 266, p.114584.

Demir, U., Goksu, C., Unal, G., Green, M. and Ilki, A. (2020). Effect of fire damage on seismic behavior of cast-in-place reinforced concrete columns. Journal of Structural Engineering, 146(11), p.04020232.

Chang, Y.F., Chen, Y.H., Sheu, M.S. and Yao, G.C. (2006). Residual stress–strain relationship for concrete after exposure to high temperatures. Cement and concrete research, 36(10), pp.1999-2005.

Tao, Z., Wang, X.Q. and Uy, B. (2013). Stress-strain curves of structural and reinforcing steels after exposure to elevated temperatures. Journal of Materials in Civil Engineering, 25(9), pp.1306-1316.

Ni, S. and Birely, A.C. (201)8. Post-fire seismic behavior of reinforced concrete structural walls. Engineering Structures, 168, pp.163-178.

Parsons, T., Toda, S., Stein, R.S., Barka, A. and Dieterich, J.H. (2000). Heightened odds of large earthquakes near Istanbul: an interaction-based probability calculation. Science, 288(5466), pp.661-665.

Erdik, M., Aydinoglu, N., Fahjan, Y., Sesetyan, K., Demircioglu, M., Siyahi, B., Durukal, E., Ozbey, C., Biro, Y., Akman, H. and Yuzugullu, O. (2003). Earthquake risk assessment for Istanbul metropolitan area. Earthquake Engineering and Engineering Vibration, 2, pp.1-23.

Zhu, M., McKenna, F. and Scott, M.H. (2018). OpenSeesPy: Python library for the OpenSees finite element framework. SoftwareX, 7, pp.6-11.

Turkish Building Seismic Code (2007). The Ministry of Public Works and Settlement, Ankara, Turkey.

Mander, J.B., Priestley, M.J. and Park, R. (1988). Theoretical stress-strain model for confined concrete. Journal of structural engineering, 114(8), pp.1804-1826.

Wallace, J.W. (2012). Behavior, design, and modeling of structural walls and coupling beams—Lessons from recent laboratory tests and earthquakes. International Journal of Concrete Structures and Materials, 6, pp.3-18.

Pugh, J.S., Lowes, L.N. and Lehman, D.E. (2015). Nonlinear line-element modeling of flexural reinforced concrete walls. Engineering Structures, 104, pp.174-192.

Gogus, A. and Wallace, J.W. (2015). Seismic safety evaluation of reinforced concrete walls through FEMA P695 methodology. Journal of Structural Engineering, 141(10), p.04015002.

Turkish Building Seismic Code (2018). Disaster and Emergency Presidency, Ankara, Turkey.

ACI (2014) ACI 318-14: Building code requirements for reinforced concrete. American Concrete Institute, Farmington Hill, USA.

Buchanan, A.H. and Abu, A.K. (2017). *Structural design for fire safety*. John Wiley & Sons.

BS EN 1991. 1-2: 2002 Eurocode 1: Actions on structures—Part 1-2: General actions—Actions on structures exposed to fire. British Standards.